CO adsorption on doped MgO(100) surface: A theoretical study by DFT cluster embedding

Carlos Quintanar [a, b], V.M. Castaño
a Centro de Física Aplicada y Tecnología Avanzada
Universidad Nacional Autónoma de Méxic
A.P. 1-1010, Querétaro, Qro., 76000, México
b Facultad de Ciencias, Universidad Nacional Autónoma de México,
Ciudad Universitaria, 04510 México D.F., México

Reyna Caballero[c]
Departamento de Supercómputo,
DGSCA, Universidad Nacional Autónoma de México
Ciudad Universitaria, 04510 México D.F., México

A density functional cluster embedding approach is applied to study the influences of the impurities in CO adsorption on the MgO surface. A 60-atom cluster centered at the impurity site and embedded in an array of 1680 point charges, models the doped MgO(100) surface. Cr and Ni substitutional impurities are studied in terms of their influence to the adsorption of CO on the MgO surface. The relaxations of the impurities are evaluated as well. The calculations show, that the doped surface has a larger CO-surface adsorption energy than the clean surface, 80% and 280% for Cr and Ni respectively. They predict also a bulk-ward relaxation of 0.02 for Ni, and an outwards relaxation of 0.025 for Cr.

1. Introduction

The interaction of CO with a MgO(100) surface, has received a great deal of attention in the literature [1]-[18]. It is considered a prototypical system for adsorption studies [15]. Moreover, since a number of metal oxides exist naturally in rocks and minerals exposed to groundwater and their presence influences the mobility of pollutants, the adsorption properties of this oxide have a geochemical relevance.

In spite of important work done in the area, the MgO-CO system is still far from to be fully understood. In particular, for the adsorption energy, has not been established a reasonable agreement between theory and experiment. Some reasons for this are: experimentally it is difficult to prepare free structural defect MgO surface, not to say free from metal impurities, which might dramatically change the interaction between the MgO surface and the CO, as will be shown in this work, on the theoretical side, poor basis set description for the surface and for the adsorbate, and reported values that were not corrected from the basis set superposition error were the common failures of the early theoretical work.

The time development of experimental and theoretical values of CO adsorption energy on the regular MgO(100) surface, published between 1978 and 2005, is shown in Figure 1. Here can be seen that, from 1987 to 1996 theoretical and experimental reported values had opposite trends. Early experiments gave low CO-MgO adsorption energies, 3.5 - 3.9 kcal/mol [1], [2], whereas later experiments provide much larger values Henry et al. 9.7 kcal/mol [3], and He et al. using thermal desorption spectroscopy (TDS) reported a value of 10.6 kcal/mol [4]. On the other hand, theoretical values obtained in 1984 by

Colbourn and Makrodt [5] and Pope et al. [6] gave a value of 8.8 kcal/mol, for the CO-MgO adsorption energy, where as the later calculations of Pacchioni and Bagus [7] in 1993 using a $Mg_{21}O_{21}$ cluster obtained a value of 5.3 kcal/mol without basis set superposition error correction (BSSE). With he same system after BSSE correction they obtain a lower value of 3.9 kcal/mol [7]. Also, they did calculations with a larger cluster $Mg_{21}O_{21}$ and obtained a BSSE corrected value of 1.8 kcal/mol[7]. In 1995 Neyman et al. using a Density Functional Theory (DFT) embedding cluster approach, reported a BSSE corrected value of 2.5 kcal/mol [8]. In 1996 Nygren and Pettersson using an ab-inito cluster reported a BSSE corrected value of 1.8 kcal/mol [10]. In 1997 Yudanov et al., using a cluster model, where the point charge embedding were substituted by a total ion model potential, obtained a value of 1.1 kcal/mol [9].

Nygren and Pettersson in their 1996 work, pointed out to the existing ´serious discrepancy´ between theoretical and experimental descriptions of the CO interaction with MgO. They also studied the published experimental and theoretical works and from those investigations they concluded that there were "a much higher density of defects or low-coordinated sites at the oxide surfaces than what is normally assumed". In other words, in the experimental situation, many low-coordinate and impurity sites were involved instead of the regular and fully coordinated sites which had been studied theoretically.

The Nygren and Pettersson claims, motivated the Freund group to undertake the one of the finest experiment ever done in this field. Through TDS experiments, using metal oxide single crystals cleaved in vacuum, they attained the smallest experimentally accessible defect density, and thus the adsorption studies were not notably
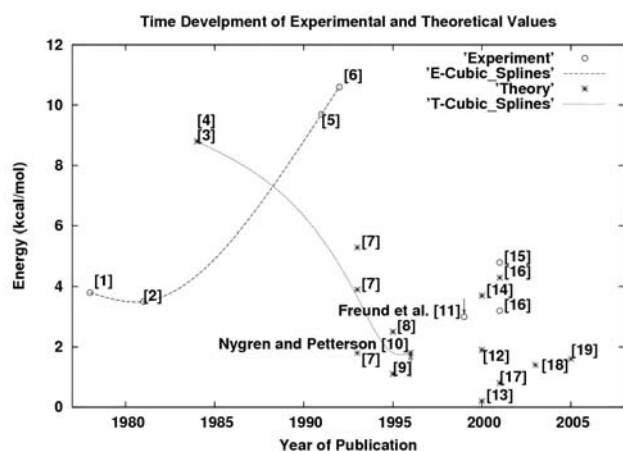
Figure 1. Time development of experimental and theoretical values of CO-MgO adsorption energy.

influenced by the interaction of adsorbates with the defects or low coordinate sites. With all those cares a CO adsorption energy of 3.0 kcal/mol was obtained [11]. This value is pointed with an arrow. In 2001, using epitaxially grown films and TDS Dohnalek et al. [15] obtained a value of 4.8 kcal/mol, by the same techniques Rodriguez et al [16] obtained the value of 3.2 kcal/mol.

After the experiments of the group of Freund, the reported theoretical values for the CO-MgO adsorption energy agreed with the value of 3.0 kcal/mol within the accepted accuracy of the used methods (~ 2 kcal-mol), as can be seen form Figure 1. In year 2000, using slabs DFT-FLAPAW with the General Gradient Approximation (GGA) of Becke-Perdew-96, Snyder [12] reported the BSSE corrected value of 1.9 kcal/mol. Sallabi

and Jack 2000 [14], applying the Monte Carlo technique obtained the value of 3.7 kcal/mol. Soave and Pacchioni 2000, using a cluster and DFT-B3LYP obtained the BSSE corrected value of 0.2 kcal/mol [13]. Damin et al. 2001, using a DFT BSSE Cluster and the functional B3LYP obtained the value of 0.8 [17], Rodriguez et al. 2001, performed theoretical calculation using a slab and DFT and the BLYP functional without correcting the BSSE, obtaining a value of 4.3 kcal/mol. [16]. Xu et al. 2003, using a DFT-GGA-B3LYP-Cluster BSSE, obtained the value of 1.4 kcal/mol [18]. In a previous work 2005, using a $Mg_{30}O_{30}$ DFT cluster with the GGA approximation of PW86 and an IGLO-III basis set for the CO, we reported the BSSE corrected value of 1.62 kcal/mol [19].

However, there is still a small discrepancy between the average of the calculated values and the average of experimental values, indicating that surface defects might still interfere with the experimental results, and that a better description for surface and the atoms direct involved in the adsorption may be needed.

The aim of this present work is to study the CO adsorption on doped MgO(100):Ni and MgO (100):Cr, by using a surface model, taking into account relaxation and rumpling.

Although these structural characteristics are experimentally well known [21], [22], [23], they are usually disregarded. The results will be compared to experimental data.

Accordingly, we first review the cluster model and the half-Evjen-cube construction method. We then proceed to studying the behavior of the Madelung potential and electron densities at the cluster surface. Finally, adsorption of CO on a Mg site, located at the center of the cluster (a five coordinated terrace) and adsorption of CO on Mg sites,

Table 1. Structural characteristics and binding energies of CO adsorbed (C over Mg) on MgO(100), MgO:Ni(100), and MgO:Cr(100) surface calculated in the LSDA approximation. Equilibrium distances for C-O, Mg-C, Cr-C, and Ni-C. The impurity (Ni, Cr) was located at a Mg site at the center of MgO sharp (S), relaxed and rumpled surface (RR).

System	Adsorbate	C-O (Å)	Metal-C[a] (Å)	Adsorption Energy (kcal/mol)	Difference (%)
MgO S	CO	1.144	2.316	9.87	
MgO RR	CO	1.145	2.329	11.16	11.6
MgO:Cr S	CO	1.161	1.988	17.77	
MgO:Cr RR	CO	1.159	1.990	21.53	17.5
MgO:Cr OPT[b]	CO	1.159	1.990	20.9	
MgO:Ni S	CO	1.154	1.794	38.10	
MgO:Ni RR	CO	1.153	1.795	38.55	1.2
MgO:Ni OPT[b]	CO	1.153	1.796	38.04	
Free CO					
LSDA.			1.145		
Exp. [12]			1.128		

[a] Mg in MgO, Cr in MgO:Cr, and Ni in MgO:Ni.
[b] For the relaxed and rumpled surface the position of the impurity in the direction normal to the surface was optimized, keeping all other cluster ions fixed.
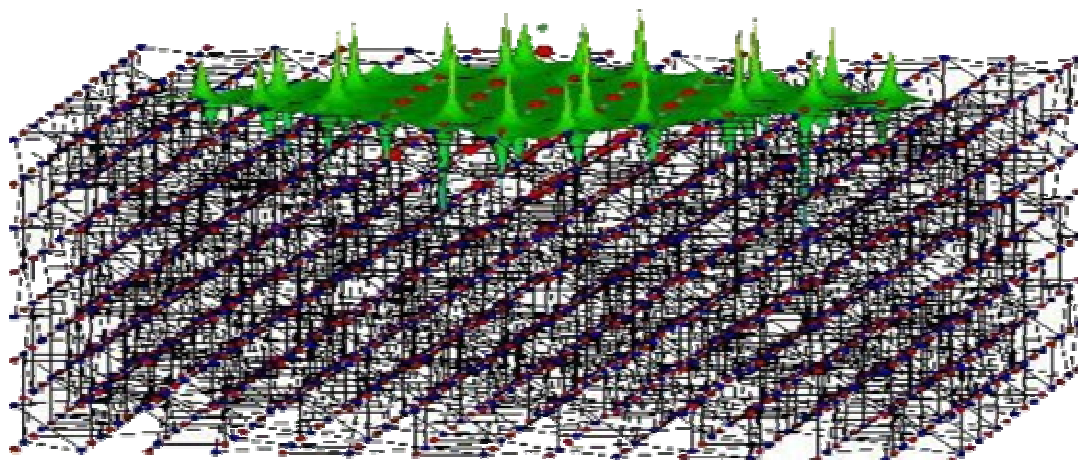
Figure 2. The sheet with spikes corresponds to the Madelung potential produced by the embedding of point charges; the larger dots represent the atoms of the embedded cluster and the smaller dots correspond to the point charges.

where the Mg is replace by an impurity like the Ni^{2+} and Cr^{2+} ions are studied.

2. Cluster model, and Evjen cube construction method

In the present study, a $Mg_{30} O_{30}$ cluster models the regular surface Mg site of MgO (100). To model the sharp surface, the Mg-O distance was taken from the experimental MgO bulk geometry (2.105 Å) [24] The Madelung potential for bulk is built up by placing positive and negative point charges, with a value of ± 2.0, at the lattice sites. In the case of the crystals of a cubic system like MgO, the weights assigned to the charges are 1, 1/2, 1/4, or 1/8, according to their location in the interior, at the face, edge, or corner of the cube. Of course, the total charge of the cube is zero. This is known as the Evjen summation method [25]. To build the Madelung potential for the surface, a variant of this method is used. Starting from the Evjen cube point charge array for the bulk, all the point charges above the surface that includes the Mg site at the center of the cube are deleted, leaving a half cube with zero total charge (see Figure 2). The point charge array used for the embedding contains 1680 point charges. The $Mg_{30} O_{30}$ clusters employed to model the sharp and relaxed-rumpled MgO (100) surfaces are shown in Figure 3.

3. Quantum chemical methods

Calculations were performed using the deMon program [26]. The local spin density approximation (LSDA) proposed by Vosko, Wilk and Nusair [27,28] and the general gradient approximation (GGA) proposed by Perdew and Wang (PW86) [29] have been applied. The exchange-correlation potential was numerically integrated on an adaptive grid [30]. The Coulomb energy was calculated by the variational fitting procedure proposed by Dunlap, Connolly, and Sabin [31, 32]. In the calculations, all electrons were treated explicitly, and the MgO(100) cluster atoms were described using the valence double-zeta plus polarization (DZVP) basis sets, (6321/411/1*) for magnesium and (621/41/1*) for oxygen, optimized for

local functionals [33]. The CO molecule was described using DZVP or IGLO (individual gauge for localized orbitals) basis sets. In studying the convergence of the CO geometrical properties, and MgO(100)-CO adsorption energy with the basis sets size, the basis set for the CO was increased from DZVP to IGLO-II (51111/2111/1) and IGLO-III (5111111/211111/11). All adsorption energies were corrected with respect to basis set superposition errors.

We report the results for the MgO(100)-CO adsorption energy, and the C-O distance obtained when the CO was described using the DZVP basis (621/41/1*) for carbon and oxygen (seven shells), and when it was described using the IGLO-III basis sets (5111111/211111/11) for carbon and oxygen (fifteen shells). Although IGLO basis sets are used to calculate properties involving an external magnetic field, which is not our case, it has been empirically proven that IGLO basis sets are sensitive to changes in geometry [34].

A quasi-Newton method [35] with analytic energy gradients was used for the structure optimization. To calculate the first nearest neighbor distance, an MgO-33-atom cluster embedded in an Evjen cube, was used to model bulk MgO.

4. Results and Discussion

The LSDA is recognized to be reliable in predicting geometries and bond lengths for a variety of materials [36]. Therefore, it was chosen to determine the structural characteristics such as C-O distance, MgO-CO distance and angles LSDA was used. LSDA density functional approximation, and cluster embedding approach are reliable in studying properties of rocksalt-like ionic crystals [35]. However, LSDA performs less effectively in predicting energies due to the inherent limitation of this approximation. Hence, for obtaining reliable information on energies, GGA of Perdew Wang PW86 has been adopted.

Table 2. Structural characteristics and binding energies of CO adsorbed (O over Mg) on MgO(100), MgO:Ni(100), and MgO:Cr(100) surface calculated in the LSDA approximation. Equilibrium distances for C-O, Mg-C, Cr-C, and Ni-C. The impurity (Ni, Cr) was located at a Mg site at the center of MgO sharp (S), relaxed and rumpled surface (RR).

System	Adsorbate	C-O (Å)	Metal[a]- O (Å)	Adsorption Energy (kcal/mol)	Difference (%)
MgO S	OC	1.145	2.309	-4.77	
MgO RR	OC	1.145	2.284	-6.20	23.0
MgO:Cr S	OC	1.164	2.202	-4.46	
MgO:Cr RR	OC	-	-	-	
MgO:Ni S	OC	1.145	2.396	-6.47	
MgO:Ni RR	OC	1.145	2.330	-7.67	15.6

[a] Mg in MgO, Cr in MgO:Cr, and Ni in MgO:Ni.

4.1. *Madelung potential, and charge densities*

The Madelung potential produced by the half-Evjen-cube was calculated, as shown in Figure 2. Here, the cluster (larger dots) can be seen embedded in an half Evjen cube point charge array (smalldots). The peaks there represent the Madelung potential produced by the Evjen cube at a point charge. In the figure, the ions at the cluster surface (larger dots) are located in a region where the Madelug potential is flat (i.e., constant).

The electron density and the electron density contour map for the cluster model, in the plane containing the fourfold symmetry axis, the O-Mg-O unit, and the CO adsorbate on top of Mg was calculated, as shown in Figure 3. Here, in the electron density contour map (on the right), the densities of the first and second nearest neighbors of the Mg site, where the CO is adsorbed, are basically undisturbed by the point charges array. The more distant neighbors (third and four), that were included in the cluster to screening the cluster inner region from the excessive interaction arising from the point charges, show some distortions. On the other hand, in the electron density (on the left) we can observe that the ions have a spherical symmetry, the small and large spheres correspond to the Mg and O ions respectively. The ionic radii agrees roughly with the values $r_{Mg} = 0.74$ and $r_O = 1.36$ reported by Belov-Bokii [37].

4.2. *MgO (100) surface relaxation an rumpling*

The accepted model for the MgO(100) surface [36] corresponds to an inward relaxation of the surface plane of no more of few percent and rumpling of the surface of less than 2% of the interplanar spacing (with the oxygen ions displacing more bulk-ward than the magnesium ions).

Early experimental results on surface rumpling and relaxation [38], [39] are scattered [19], [18], [21], [22], possibly due to the presence of surface contaminants such as water, oxygen and a high amount of surface defects [18]. However, a consistent picture emerges from the most recent measurements of Medium-Energy Ion-Scattering MEIS [40], Grazing Incidence X-ray Scattering GIXS [41], and Low Energy Electron Diffraction LEED [21], where great care has been taken as to ensure the quality of the

surfaces. For this reason, this experimental data will be taken as reference. In these works the relaxation range from -2.0 ±0.7 to 1.0 ±1.0%, and the rumpling form 0.5 ±1.0 to 3.3 ±1.5%. In a previous work [19], the relaxation and rumpling of the MgO (100) surface and the values we have obtained were -1.4% and 0.95% for the relaxation and rumpling respectively. These values agree reasonably with the experimental data above. For this reason, this surface will be used as model to study the CO adsorption on the impurified MgO:Ni(Cr)(100) surface.

Surface relaxation δd_{rel} is defined as the difference of the averaged vertical distance from the first layer of atoms to the second layer d_{12} from the bulk inter-layer spacing **d**, and it is reported as percentage of *d*. (see Figure 4).

$$\delta d_{rel} = [(d_{12} - d)/d]*100\%$$

Surface rumpling Δ_{rum} is defined as the difference of the mean vertical position of oxygen z_1^O and the magnesium z_1^{Mg} atoms in the first layer, and it also is given as percentage of *d*. (see Figure 4).

$$\Delta_{rum} = [(z_1^O - z_1^M)/d]*100\%$$

4.3. *CO adsorption on MgO surface*

Structural characteristics and adsorption energies of CO adsorbed on MgO(100), MgO:Ni(100), and MgO:Cr(100) surface calculated in the LSDA approximation are in Table I. Here, that metal-C distances decrease, according to the sequence MgO > (MgO:Cr) > (MgO:Ni). However, the C-O distance increases with respect to the free molecule 1.45Å distance, following the sequence MgO < (MgO:Ni) < (MgO:Cr). The increases may be related to a weakening of the bond.

By freeing the metal impurity along the normal to the surface, while keeping all other cluster atoms fix, the impurity position was optimized. It was found that Ni moves 0.02 Å bulk-wards, whereas Cr moves 0.025 Å from the bulk, producing a negligible change in the adsorption energy, as can be seen in Table 1. (rows "Cr optimized[b]" and 'Ni optimized[b]").

The CO adsorption with O on top of Mg (metal-O) was explored as well, Table 2. It can be observed, that the adsorption energy decreases drastically (as compared to C
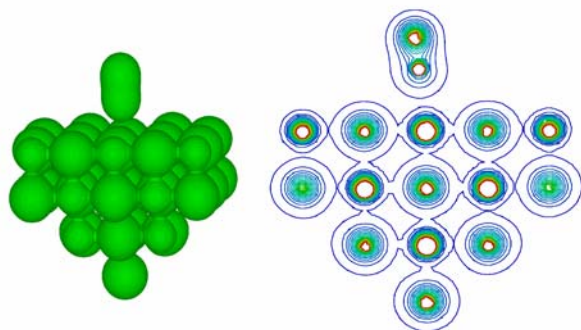
Figure 3. Electron density and the electron density contour map in the plane containing the fourfold symmetry axis, the O-Mg-O unit, and the C-O above the Mg ion.

Figure 4. The Cluster models for the sharp and relaxed-rumpled MgO(100) surfaces.

on top of Mg), from 9.87 kcal/mol to 4.77 kcal/mol, for MgO; from 17.77 to 4.46 kcal/mol, for MgO:Cr; and from 38.10 kcal/mol to 6.47 kcal/mol for MgO:Ni.

By using the relaxation and rumpling obtained using the LSDA approximation, the geometry of MgO-CO system was optimized through the GGA PW86 approximation and the results are shown in (Table 3, in the rows 'PW86^b'). Here, the structural characteristics obtained for metal-C distances and C-O distances, using the functional PW86 show the same trend as that of LSDA. Table 3 rows 'LSDA' show the LSDA optimized values; rows 'PW86^b' show the geometries and energies calculated having the MgO surface with the LSDA relaxation and rumpling, but optimizing the MgO-CO, MgO:Cr-CO and MgO:Ni-CO systems; row 'PW86^b BSSE' show the basis set superposition error (BSSE) corrected adsorption energy for the CO adsorption on MgO using a dzvp basis set; row 'PW86^b BSSE-IGLO' show the basis set superposition error (BSSE) corrected adsorption energy for the CO adsorption on MgO using dzvp for the MgO cluster while IGLO-III for the CO.

In rows 'Exp.' experimental values reported in the literature are shown. It can be observed that the absorption energies for the general gradient approximation PW86^b, PW86^b BSSE and PW86^b BSSE-IGLO; $E_{PW86}{}^b$=5.73, $E_{PW86}{}^b{}_{BSSE}$=0.0 and $E_{PW86}{}^b{}_{BSSE-IGLO}$ =1.62 kcal/mol shown in Table 3, agree fairly with the experimental results, within the accepted accuracy for the DFT-GGA adsorption energy prediction, 5.0 kcal/mol [16], [43], [44], [45]. The best adsorption energy prediction so far $E_{PW86}{}^b{}_{BSSE-IGLO}$ 1.62 kcal/mol, was produced by the calculation where the CO electrons were described using an IGLO-III basis set.

The LSDA, PW86 and PW86^b adsorption energies show the same trend $E_{MgO} < E_{MgO:Cr} < E_{MgO:Ni}$. All structural characteristics obtained using the GGA PW86 show the same trend as the obtained with LSDA. Finally, as expected, LSDA overestimates the adsorption energy. Table 1 and 3 show how Ni and Cr impurities increase the adsorption energy up to 280% and 80%, respectively.

5. Conclusions

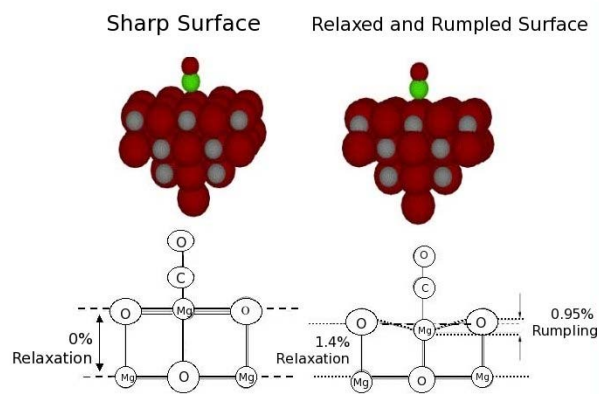Adsorption energies increase over than 10% when the rumpling and relaxation for the MgO surface are taken into account.

Considering both our results and the results reported in the literature for the pure MgO (100), we can observe that there is still a small discrepancy between the theoretical and experimental adsorption energies. The best experimental value is 3.0 kcal/mol whereas the theoretical values average around 2.0 kcal/mol. Taking into account this, we found an increase of the adsorption energy from 0.0 to 1.62 kcal/mol when the description of the ions involved in the adsorption were improved, which suggests that further improving the description of those ions might close the gap between theoretical and experimental results. Our calculations predict a CO-surface adsorption energy increase of around 80% and 280% for Cr and Ni, respectively when considered as impurities on the MgO surface. A bulkward relaxation of 0.02Å for Ni, and an outward relaxation of 0.025Å for Cr were found. These relaxations change slightly the adsorption energy value. Finally, the values obtained for the absorption of CO on MgO (100) with O on top of Mg (Mg-O), were nearly three times smaller than the Mg-C values.

References

[1] S. Furuyama, H. Fujii, M. Kawamura, T. Morimoto, J. Phys. Chem. **82**, 1028 (1978).

[2] E. A. Paukshtis, R. I. Soltanov, and N. E. Yurchenko, Reaction Kinet. Catalysis Lett. **16**, 93 (1981)

[3] C. R. Henry, C. Chapon, and C. Duriez, J. Chem. Phys. **95**, 700 (1991).

[4] J.-W. He, C. A. Estrada, J. S. Corneille, M. -Ch. Wu, and D. Wayne Goodman, Surf. Sci. **261**, 164 (1992).

[5] E. A. Colbourn and W. C. Mackrodt, Surf. Sci. **143**, 391, (1984).

[6] S. A. Pope, I. H. Hillier, M. F. Guest, E. A. Colbourn, and J. Kendrick, Surf. Sci. **139**, 299 (1984).

[7] C. Pacchioni and P. S. Bagus, in: Adsorption on Ordered Surfaces of Ionic Solids and Thin Films, Eds. H.-J. Freund and E. Umbach, Vol. 33, (Springer Series Surf. Sci., Springer-Verlag, Berlin, 1993) p. 180.

[8] K. M. Neyman, S. Ph. Ruzankin, and N. Rösch, Chem. Phys. Letters **246**, 6, 546, (1995).

[9] I.V. Yudanov, V. A. Nasluzov, K. M. Neyman, N. Rösch, Int. J. Quant. Chem. **65**, 975 (1997)

Table 3. Comparison between the LSDA, GGA(PW86), and experimental data of   distances C-O, Cr-C, and Ni-C. Adsorption energies of the MgO(100), MgO:Cr(100), and MgO:Ni(100) relaxed and rumpled surfaces. BSSE: Basis set superposition error, the adsorption energy value is corrected taking into account the basis set superposition error.

System	Method	Adsorbate	C-O (Å)	Metal –C[a] (Å)	Adsorption energy (kcal/mol)
MgO	LSDA	CO	1.145	2.329	11.2
MgO	PW86[b]	CO	1.15	2.662	5.7
MgO	PW86[b] BSSA	CO	1.15	2.662	0.0
MgO	PW86[b] BSSA-IGLO	CO	1.134	2.754	1.6
MgO	Exp.[11]	CO	-	-	3.0
MgO:Cr	LSDA	CO	1.159	1.99	21.5
MgO:Cr	PW86[b]	CO	1.166	2.124	7.8
MgO:Cr	Exp. [16]	CO	-	-	19.0
MgO:Ni	LSDA	CO	1.153	1.795	38.5
MgO:Ni	PW86[b]	CO	1.159	1.920	22.2
MgO:Ni	Exp. [16]	CO	-	-	14.0
Free CO					
CO	LSDA		1.145		
CO	PW86		1.153		
CO	PW86 IGLO		1.134		
CO	Exp. [12]		1.28		

[a] Mg in MgO, Cr in MgO:Cr, and Ni in MgO:Ni.
[b] MgO-CO optimized using the GGA PW86

[10] M. A. Nygren and L. G. M. Petterson, J. Chem. Phys., **105**, 9339, (1996).
[11] Wichtendahl, M. Rodriguez-Rodrigo, U. Härtel, H. Kuhlenbeck, and H.-J. Freund. Phys, Stat. Sol. (a) **173**, 93 (1999).
[12] J. A. Snyder, D. R. Alfonso, J. E. Jaffe, Z. Lin, A. C. Hess, and M. Gutowski, J. Phys. Chem. B, **104**, 4717 (2000)
[13] R. Soave, and G. Pacchioni, Chem. Phys. Letters, **320**, 345 (2000).
[14] K. Sallabi, and D. B. Jack, J. Chem. Phys., **112**, 5133 (2000).
[15] Z. Dohnálek, G. Kimmel, S. A. Joyce, P. Ayotte, R. S. Smith and B. D. Kay, J. Phys. Chem B **105**, 3747 (2001).
[16] J. A. Rodriguez, T. Jirsak, M. Perez, L. Gonzalez, A. Maiti, J. Chem. Phys. **114**, 4186 (2001).
[17] Damin, R. Dovesi, A. Zecchina, P. Ugliengo, Surf. Sci. **479**, 255 (2001).
[18] Y. Xu, J. Li, Y. Zhang, and W. Chen, Surf. Sci. **525**,13 (2003).
[19] C. Quintanar, R. Caballero, and V. M. Castaño, Int. J. Quant. Chem. **102**, 820 (2005).
[20] G. Benedek, G. Brusdeylins, V. Senz, J. G. Skofronick, J. P. Toennies, Traeger, and R. Vollmer, Phys. Rev. B **64**, 125421 (2001).
[21] D. Ferry, J. Suzanne, V. Panella, A. Barbien, M. A. Van Hove, and J.-P. Bibérian, J. Vac. Sci. Technol. A **16**, 2261 (1998).
[22] D. R. Alfonso, J. A. Snyder, J. E. Jaffe, A. C. Hess,and M. Gutowski, Phys. Rev. **62**, 8318 (2000).
[23] N. W. Ashcroft and N. David Mermin, Solid State Physics,Holt, Rinehart and Wiston, Holt-Saunders International Editions, (1976).
[24] H. M. Evjen Phys. Rev. **39**, 675 (1932).
[25] A.M. Köster, G. Geudtner, A. Goursot, T. Heine, A. Vela, D.R. Salahub, deMon, NRC, Canada (2002).

[26] S. H. Vosko, L. Wilk, and M. Nusair, Can. J. Phys., **58**, 1200 (1980).
[27] L. Wilk, and S. H. Vosko, J. Phys. C., **15**, 2139 (1982).
[28] J. P. Perdew, Y. Wang, Phys. Rev.B **33**, 8800 (1986).
[29] M. Krack and A. M. Köster, J. Chem. Phys. **108**, 3226 (1998).
[30] B. I. Dunlap, J. W. D. Connolly, and J. R. Sabin, J. Chem. Phys. **71**, 4993 (1979).
[31] J. W. Mintmire and B. I. Dunlap, Phys. Rev. A 25, 88 (1982).
[32] N. Godbout, D. R. Salahub, J. Andzelm, and E. Wimmer, Can. J. Phys. **70**, 560 (1992).
[33] H. B. Schlegel, J. Comput. Chem. **3**, 214 (1982).
[34] Kutzelnigg, W.; Fleisher, U.; Schindler, M. In NMR Basic Principles and Progress; Diehl, P.; Fluck, E.; Gunther, H.; Kosfeld, R.; Seelig, (J., Eds.; **23**; Springer: Heidelberg 1990), p. 165.
[35] C. Quintanar, R. Caballero, and A. M. Koster, Int. J. Quant. Chem. **96**, 483 (2004).
[36] D. R. Alfonso, J. A. Snyder, J. E. Jaffe, A. C. Hess,and M. Gutowski, Phys. Rev. **62**, 8318 (2000).
[37] Crystal Physics, A. F. Brown, Trans. –Ed., Academy Press.
[38] Santoni, D. B. Thoai, and J. Urban, Solid State Communications. **68**, 1039 (1988).
[39] H. Naskamatsu, A. Sudo, S. Kawai, Surf. Sci **194,** 265 (1998)
[40] J. B. Zhou, H. C. Lu, T. Gustafsson and P. Häberle, Surf. Sci. **302**, 350 (1994).
[41] O. Robach, G. Renaud, A. Barbier, Surf. Science **401**, 227 (1998).
[42] D. C. Sorescu. C. N. Rusu, and J. T. Yates, J. Phys. Chem, B **104**, 4408, (2000).
[43] T. Ziegler, Chem. Rev. **91**, 651 (1991), R. A. vam Santen, and M. Newrock, Catal. Rev. Sci. Eng **37**, 557, (1995).
[44] D. C. Sorescu and J. T. Yates, J. Phys. Chem. B **102**, 4556 (1998).